

Supporting Information

Bright Near-Infrared Circularly Polarized Electrochemiluminescence from Au₉Ag₄ Nanoclusters

List :

Synthesis and purification

Characterizations and measurements

Supplementary schemes

Scheme S1. ECL mechanistic pathways with 50 mM TPrA.

Scheme S2. ECL mechanistic pathways with 100 mM TPrA.

Scheme S3. ECL mechanistic pathways with 300 mM TPrA.

Scheme S4. ECL mechanistic pathways with 700 mM TPrA.

Supplementary Figures

Figure S1. XPS survey spectrum of Au₉Ag₄.

Figure S2. ¹H NMR spectrum of Au₉Ag₄.

Figure S3. ³¹P NMR spectrum of Au₉Ag₄.

Figure S4. TGA of Au₉Ag₄.

Figure S5. XPS survey spectrum of *S*-Au₉Ag₄ and *R*-Au₉Ag₄.

Figure S6. Fluorescence lifetime of Au₉Ag₄, *S*-Au₉Ag₄, and *R*-Au₉Ag₄.

Figure S7. Photon energy spectrum of *R*-Au₉Ag₄ and *S*-Au₉Ag₄.

Figure S8. Reductive-oxidation ECL of *S*-Au₉Ag₄ with various amount of BPO coreactant.

Figure S9. Oxidative-reduction ECL of *S*-Au₉Ag₄ with various amount of TPrA coreactant.

Figure S10. Oxidative-reduction ECL of *R*-Au₉Ag₄ with various amount of TPrA coreactant.

Figure S11. CV of *S*-Au₉Ag₄ and *R*-Au₉Ag₄.

Figure S12. PL spectra of *S*-Au₉Ag₄ under electrolysis and ECL spectra of *S*-Au₉Ag₄ with various concentration of TPrA coreactant.

Figure S13. PL intensities of *S*-Au₉Ag₄ nanoclusters under various potential electrolysis conditions.

Figure S14. Diagram of apparatus for CPECL measurement with the commercial CPL instrument.

Figure S15. Diagram of apparatus for CPECL measurement with the Andor camera and spectrometer with polarizers.

Figure S16. Six groups of ECL spectra of *S*-Au₉Ag₄ without or with CPIL808/ CPIR808 polarizer.

Figure S17. Six groups of ECL spectra of *R*-Au₉Ag₄ without or with CPIL808/ CPIR808 polarizer.

Figure S18. Six groups of ECL spectra of *S*-Au₉Ag₄ before and after adding 1 equivalent of *S*-CPA.

Figure S19. Six groups of ECL spectra of *S*-Au₉Ag₄ before and after adding 1 equivalent of *R*-CPA.

Figure S20. Six groups of ECL spectra of *R*-Au₉Ag₄ before and after adding 1 equivalent of *R*-CPA.

Figure S21. Six groups of ECL spectra of *R*-Au₉Ag₄ before and after adding 1 equivalent of *S*-CPA.

Figure S22. CPL of *S*-Au₉Ag₄ and *R*-Au₉Ag₄ after added *S*-CPA and *R*-CPA.

Figure S23. CPL of *S*-Au₉Ag₄ and *R*-Au₉Ag₄ after added TPrA.

Supplementary Table

Table S1. Crystal data and structure refinement for $[\text{Au}_9\text{Ag}_4(\text{DPPB})_4\text{Cl}_4]\text{Cl}$.

Synthesis and purification

Racemic Au₉Ag₄ nanoclusters were synthesized by a one-pot method. Typically, 0.2 mmol AgNO₃ was dissolved in ethanol (25 mL), bisdiphenylphosphinobutane was added to the solution and vigorously stirred for about 10 minutes. Then, 0.2 mmol of hydrogen tetrachloroaurate and cyclohexanethiol were added into the ethanol. Quickly add NaBH₄ (0.4 mmol) dissolved in 5 ml of ethanol to the above solution. The organic phase immediately turned dark brown and was then stirred for 12 hours. Then, the ethanol was evaporated using the general purification protocol and washed with n-hexane. Finally, a red powder sample was obtained by vacuum drying. Au₉Ag₄ clusters were diffusely crystallized in a mixed solution of dichloromethane and n-hexane, and red crystals were obtained after one week.

R/S-Au₉Ag₄ nanoclusters were synthesized by using a one-pot method. Generally, 0.2 mmol AgNO₃ was dissolved in ethanol (25 mL), 0.1 mmol *S*-DIOP or *R*-DIOP (1,4-bis (diphenylphosphine) - 2,3-isopropyl-2,3-butanedione) was added into the solution under vigorously stirring. Ten minutes later, 0.2 mmol of hydrogen tetrachloroaurate and 0.3 mmol of cyclohexyl mercaptan were added into ethanol. Then, a freshly prepared solution of NaBH₄ (0.4 mmol in 5 mL ethanol) was quickly added. The organic phase immediately turns dark brown. The reaction was aged for 12 h in ambient. Then ethanol was evaporated, and the mixture was washed with n-Hexane. DCM was added to extract the nanoclusters. Finally, a red powder sample was obtained by vacuum drying.

Characterizations and measurements

UV-visible absorption spectroscopy. The UV-Vis absorption spectrum of Au₉Ag₄, *R*-Au₉Ag₄ and *S*-Au₉Ag₄ dissolved in DCM, whose background correction was made using a DCM blank.

X-ray photoelectron spectroscopy. X-ray photoelectron spectroscopy (XPS) measurements were performed on a Thermo ESCALAB 250, configured with a monochromated Al K α (1486.8 eV) 150 W X-ray source, 0.5 mm circular spot size, a flood gun to counter charging effects, and an analysis chamber base pressure lower than 1×10^{-9} mbar; and data were collected at FAT = 20 eV.

¹H NMR. ¹H NMR data were recorded on a Bruker Avance II spectrometer (400 MHz), in which ~5 mg samples were dissolved in 0.7 mL of CD₂Cl₂.

Thermogravimetric analysis. Thermogravimetric analysis (TGA) was carried out on a thermogravimetric analyzer (DTG-60H, Shimadzu Instruments, Inc.) with 10 mg Au₉Ag₄ in an Alumina (Al₂O₃) pan. Thermogravimetric analysis (TGA) of Au₉Ag₄ nanoclusters shows two steps of the mass loss upon heating from 38 °C to 800 °C. There is an additional first step in the clusters, which results from the evaporation of water molecules. However, the ligand decomposes in one step at 200 °C. For the cluster, the destruction of the organic compound is complete before 800 °C. Therefore, the residual mass of the clusters samples consists of metal atoms only 53.74 %. TGA analysis shows that the organic weight loss of the Au₉Ag₄ is 46.26% (wt.). This composition of Au₉Ag₄ clusters is further supported by the elemental analysis.

Circular dichroism. The circular dichroism (CD) spectrum was recorded in a quartz cell with a 0.1 cm optical path length using a Bio Logic MOS-500 CD spectropolarimeter. The spectrum was recorded in a dilute solution of dichloromethane, and the signal of the blank solvent was subtracted.

Circularly polarized luminescence. Circularly polarized luminescence (CPL) spectra were recorded by a JASCO CPL-300 instrument which dissolved in DCM. The parameters were set as

follows: scanning speed of 100 nm/min, Ex slit width 2000 μm , Em slit width 2000 μm , accumulations of 10. The reproducibility of CPL spectrum for each sample was confirmed by repeating the measurement for three times at least. 420 nm light was used to irradiate the sample. The parameters were set as above except the number of repetitions is once.

Electrochemical and ECL measurements. Voltammetry experiments were performed on a CHI 660e. A platinum mesh electrode was used as the working electrode. Pt foil and Ag/AgCl wire were used as counter and reference electrodes, respectively. The sample of 0.23 mM nanoclusters was dissolved in DCM containing 0.1 M TBAP and the solution was purged with argon for 20 min before the experiment. All data were collected at room temperature.

ECL measurements. ECL experiments were also performed using a three-electrode system in a quartz cuvette. 10 mg of nanoclusters were dissolved in DCM and a platinum mesh electrode was used as the working electrode. The working electrode and cuvette are aligned in a fixed position relative to the camera for consistency. Ag/AgCl wire served as the reference electrode and a Pt foil as the counter electrode. The sample solution was purged for about 20 min with argon prior to the measurements. The ECL intensity versus time was recorded with an Andor iDUS CCD camera (model No: DU401A-BR-DD) and further converted into ECL-voltage curves by Origin software. The camera was externally triggered by the potentiostat (Gamry Reference 600+) for synchronization. ECL spectra were collected with an Andor spectrograph (Kymera 193i).

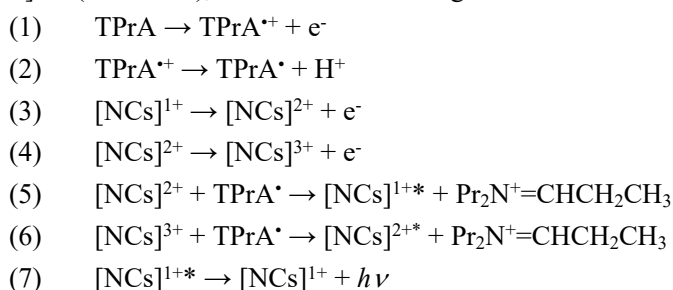
CPECL measurements. CPECL experiments were performed using a three-electrode system in a quartz cuvette. A platinum mesh electrode was used as the working electrode. The working electrode and cuvette are aligned in a fixed position relative to the camera for consistency. Ag/AgCl wire was used as reference electrode and Pt foil was used as counter electrode. All experiments were performed with TPrA as the co-reactant. The sample solution was purged with argon for about 20 minutes before measurement. A constant potential of 0 to 1.7 V vs Ag/AgCl was applied to generate ECL emission. CPECL experiments were performed on samples dissolved in DCM 0.23 mM *S/R/Rac*-Au₉Ag₄ with 700 mM TPrA and TBAP (0.1 M). The emission intensity was recorded with an Andor iDUS CCD camera (Model: DU401A-BR-DD). The cameras were externally triggered by a potentiostat (Gamry Reference 600+) for synchronization. A CPIL808 or CPIR808 polarizers were added between the quartz cuvette and the Andor spectrometer. An optical fiber was attached to the spectrometer to collect the spectra. CPECL spectra were collected with an Andor spectrometer (Kymera 193i). For the results in Figure 4a, experimental conditions were similar to the above described except for the instruments. The spectra were collected on JASCO CPL-300 instrument, in which no excited light was applied. The potentials were applied with a mini potentiostat (PalmSens EmStatBlue).

PL measurements under electrolysis. The PL spectra of various *S*-Au₉Ag₄ charge states were obtained by electrolysis at the appropriate potential of a 0.1 mM *S*-Au₉Ag₄ DCM electrolyte solution. The electrolysis was performed using a Pt mesh as the working electrode, Ag/AgCl wire was used as reference electrode and Pt foil was used as counter electrode. The samples were excited using a 405 nm laser. Spectra were acquired using an Andor iDUS CCD camera (Model: DU401A-BR-DD).

Supplementary schemes

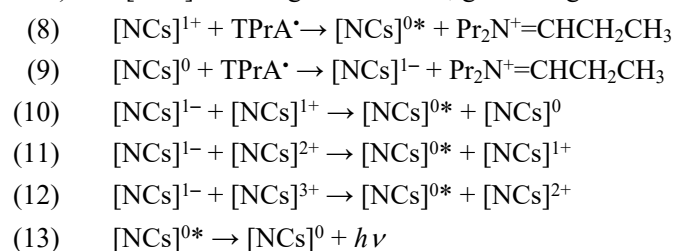
Scheme S1. ECL mechanistic pathways with 50 mM TPrA.

TPrA is an efficient coreactant that can significantly enhance the ECL of luminophores. In the presence of TPrA as coreactant, the luminophores undergo oxidative reduction pathway and generate ECL. In the presence of 50 mM TPrA, TPrA is firstly oxidized to form the TPrA radical cation, which is deprotonated to form TPrA with strong reducibility (reaction 1 and 2). [NCs] ([NCs] is *S*-Au₉Ag₄ or *R*-Au₉Ag₄) undergo oxidative processes to form [NCs]²⁺ and [NCs]³⁺ (reaction 3 and 4). The electron transfer reaction between the TPrA[•] and oxidized [NCs]²⁺ produces the excited [NCs]^{1+*} (reaction 5), which relaxes to the ground state and emits light (reaction 7, λ = 760 nm).



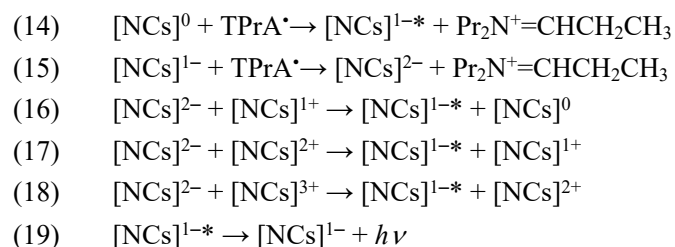
Scheme S2. ECL mechanistic pathways with 100 mM TPrA.

In the presence of high concentrations of TPrA (e.g. 100 mM), the [NCs]¹⁺ is reduced by TPrA[•] to generate excited [NCs]^{0*} (reaction 8), which emits light when it relaxes to the ground state (reaction 13, λ = 780 nm). In addition, TPrA[•] reduces the produced [NCs]⁰ to form [NCs]¹⁻ (reaction 9), and the [NCs]¹⁻ reacts with [NCs]¹⁺, [NCs]²⁺, and [NCs]³⁺, forming [NCs]^{0*} (reaction 10, 11, and 12). All [NCs]^{0*} undergo reaction 13, generating ECL.



Scheme S3. ECL mechanistic pathways with 300 mM TPrA.

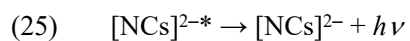
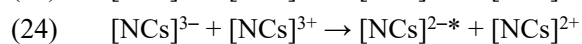
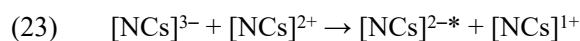
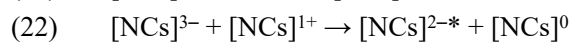
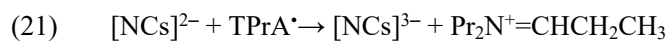
In the presence of higher concentrations of TPrA (e.g. 300 mM), the generated [NCs]⁰ is reduced by TPrA[•] to generate excited [NCs]^{1-*} (reaction 14) that relaxes to the ground state and emits light (reaction 19, λ = 790 nm). In addition, the [NCs]¹⁻ is reduced TPrA[•] to generate [NCs]²⁻, which reacts with [NCs]¹⁺, [NCs]²⁺, and [NCs]³⁺, forming [NCs]^{1-*} (reaction 16, 17, and 18). All [NCs]^{1-*} undergo reaction 19, generating ECL.



Scheme S4. ECL mechanistic pathways with 700 mM TPrA.

In the presence of very high concentrations of TPrA (e.g. 700 mM), the [NCs]¹⁻ is reduced by TPrA[•] to generate excited [NCs]^{2-*} (reaction 20), which emits light when it relaxes to the ground state and forms [NCs]²⁻ (reaction 25, λ = 805 nm). Besides, TPrA[•] reduces the generated [NCs]²⁻ to

form $[\text{NCs}]^{3-}$ (reaction 21), and the $[\text{NCs}]^{3-}$ reacts with $[\text{NCs}]^{1+}$, $[\text{NCs}]^{2+}$, and $[\text{NCs}]^{3+}$, forming $[\text{NCs}]^{2-*}$ (reaction 22, 23, and 24). All $[\text{NCs}]^{2-*}$ undergo reaction 25, generating ECL.



Supplementary Figures

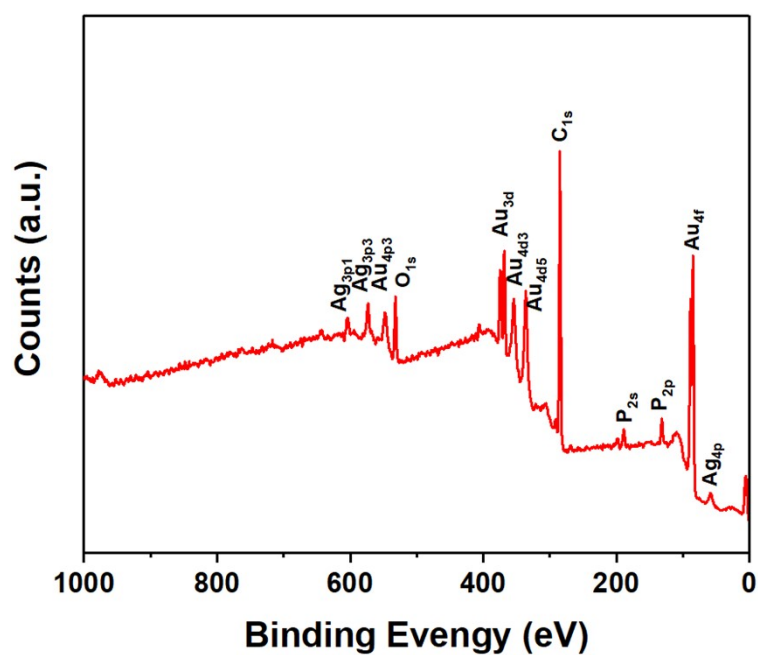


Figure S1. XPS survey spectrum of Au₉Ag₄, confirming the presence of Au, Ag, P, Cl, and C.

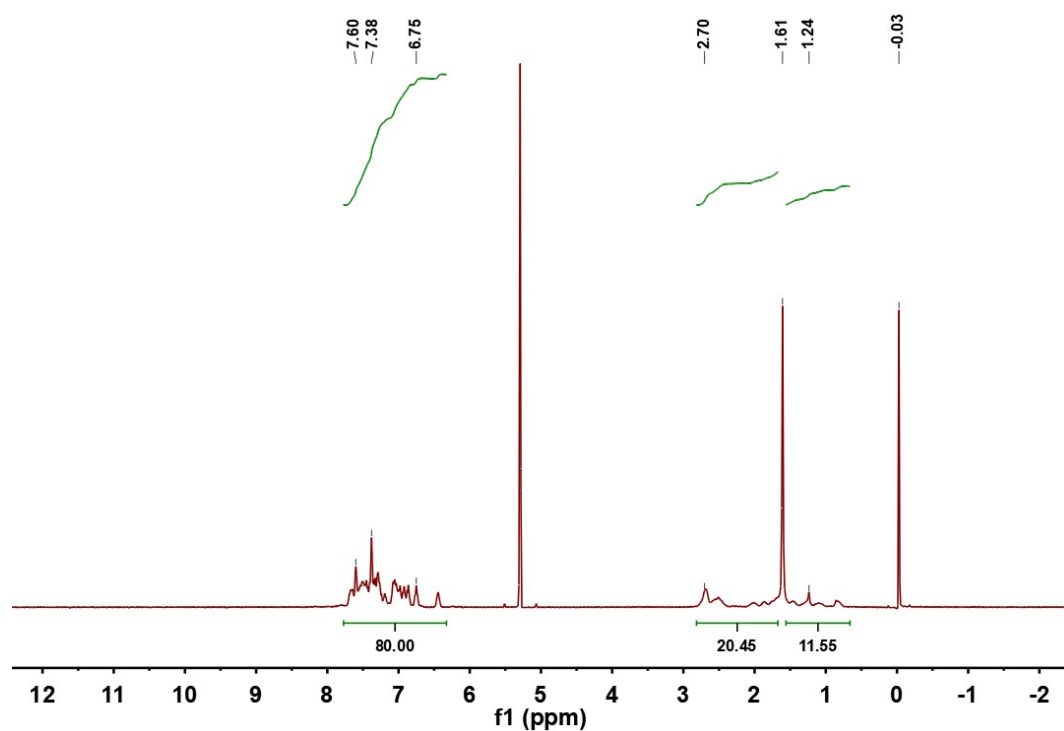


Figure S2. ¹H NMR spectrum of Au₉Ag₄ in CD₂Cl₂. Excluding the water peak, the ratio of the integral area of the alkyl group to the integral area of the benzene ring area is 80 : 32 consistent with the theoretical value.

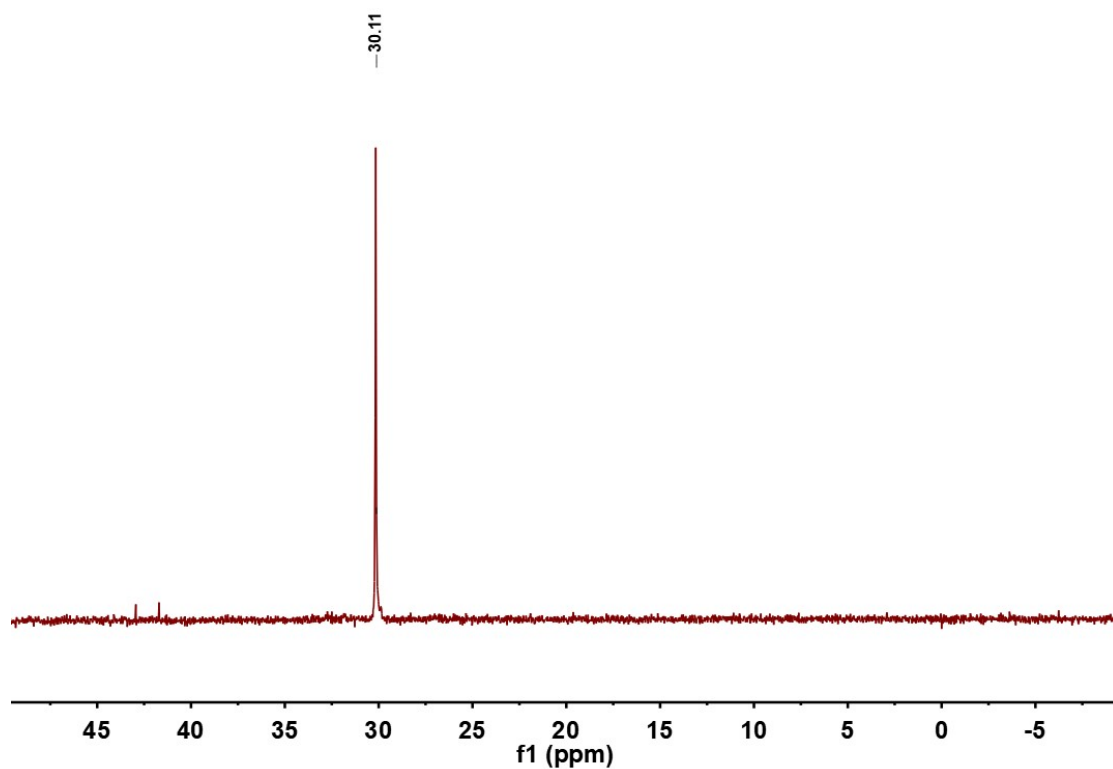


Figure S3. ^{31}P NMR spectrum of Au_9Ag_4 in CD_2Cl_2 .

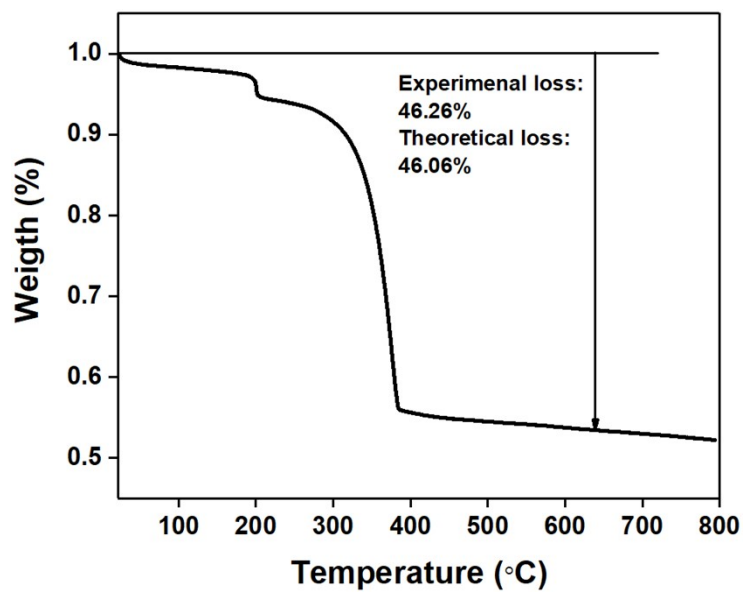


Figure S4. TGA of Au_9Ag_4 .

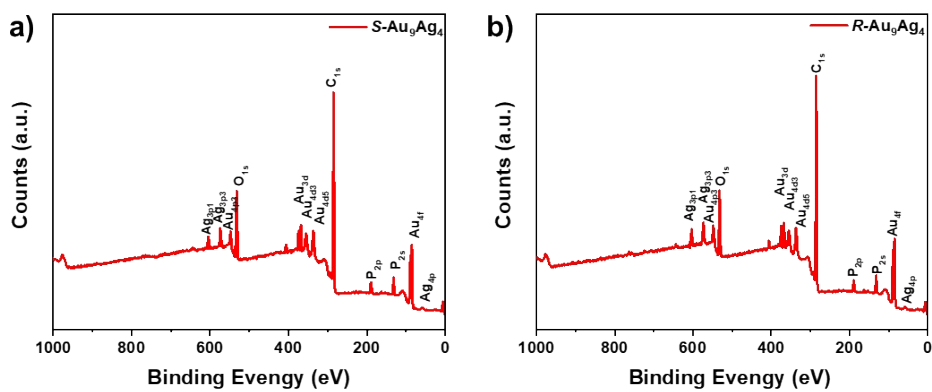


Figure S5. XPS spectra of $S\text{-Au}_9\text{Ag}_4$ and $R\text{-Au}_9\text{Ag}_4$ nanoclusters.

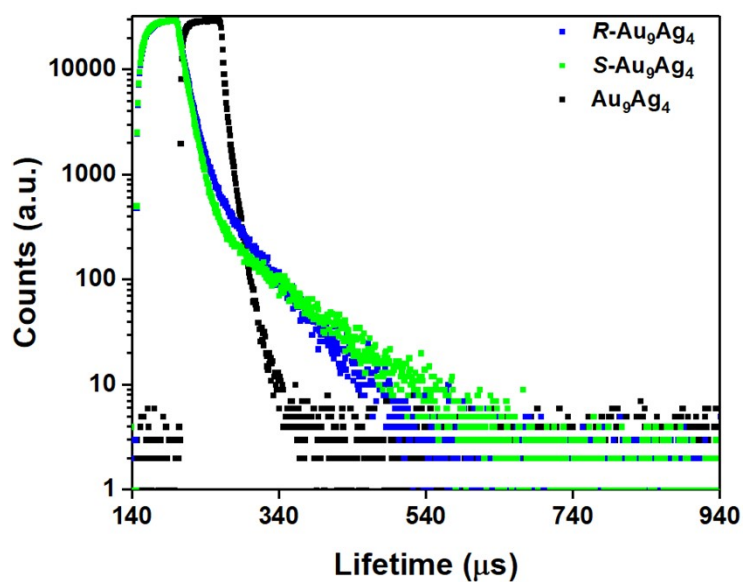


Figure S6. Fluorescence lifetime of Au_9Ag_4 (black), $S\text{-Au}_9\text{Ag}_4$ (green) and $R\text{-Au}_9\text{Ag}_4$ (blue) dissolved in dichloromethane.

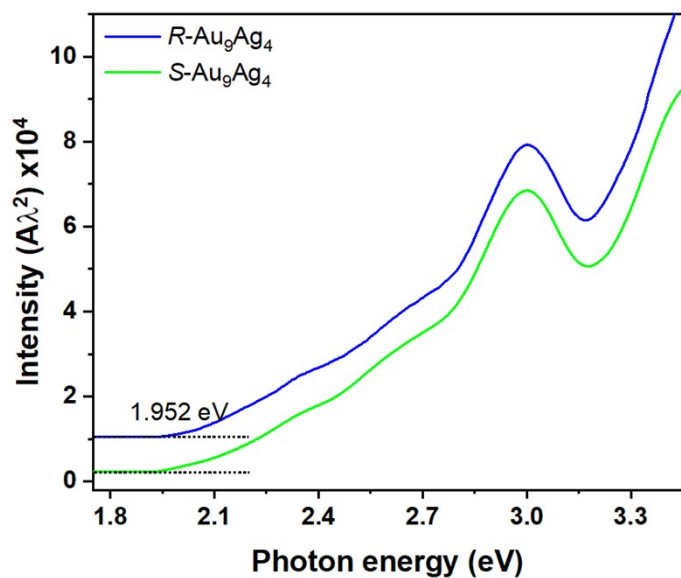


Figure S7. Photon energy spectra of $R\text{-Au}_9\text{Ag}_4$ (blue line) and $S\text{-Au}_9\text{Ag}_4$ (green line).

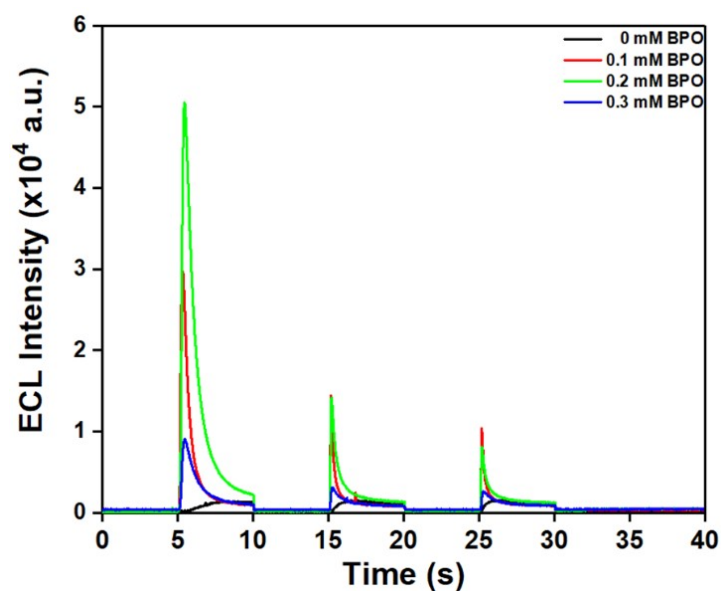


Figure S8. Reductive-oxidation ECL of $S\text{-Au}_9\text{Ag}_4$ with various amount of BPO coreactant. The electrode potential was held for 5 s in each step from -1.6 to 0 V over three cycles. The first and final 5 s provide the baseline. The exposure time was 0.02 s.

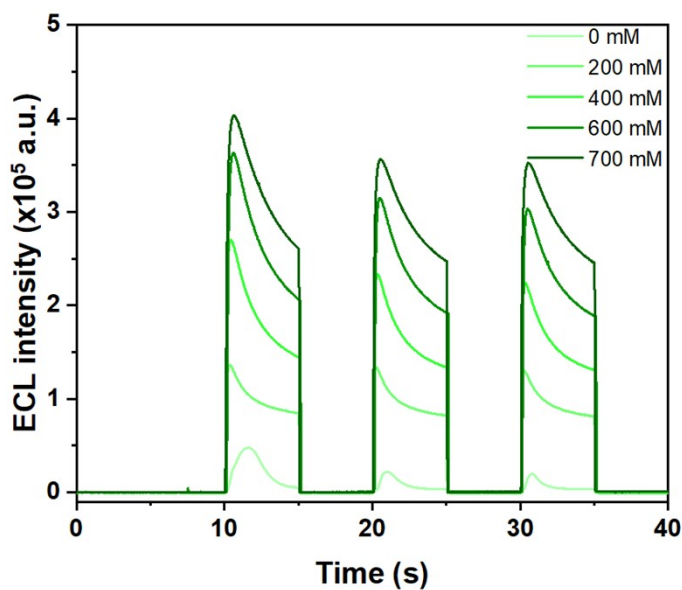


Figure S9. Oxidative-reduction ECL of *S*-Au₉Ag₄ with various amounts of TPrA coreactant. The electrode potential is held for 5 s in each step from 0 to 1.7 V over three cycles. The first 5 s and last 5 s provide the baseline. The exposure time was 0.02 s.

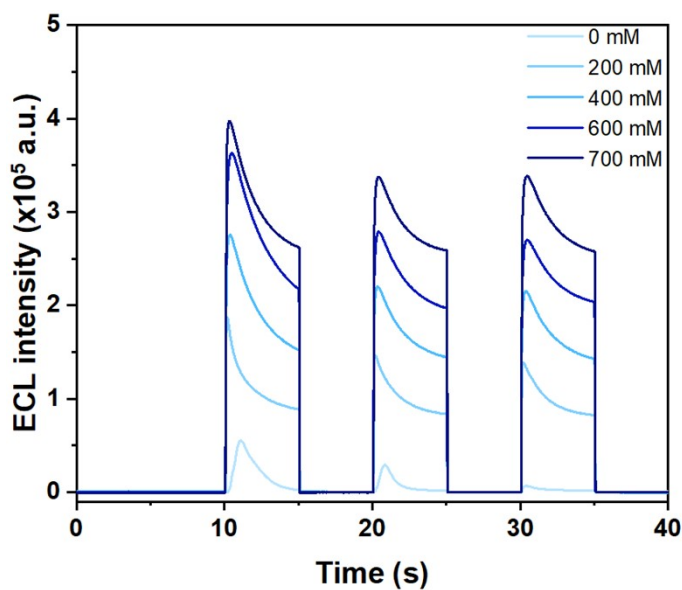


Figure S10. Oxidative-reduction ECL of *R*-Au₉Ag₄ with various amounts of TPrA coreactant. The electrode potential is held for 5 s in each step from 0 to 1.7 V over three cycles. The first 5 s and last 5 s provide the baseline. The exposure time was 0.02 s.

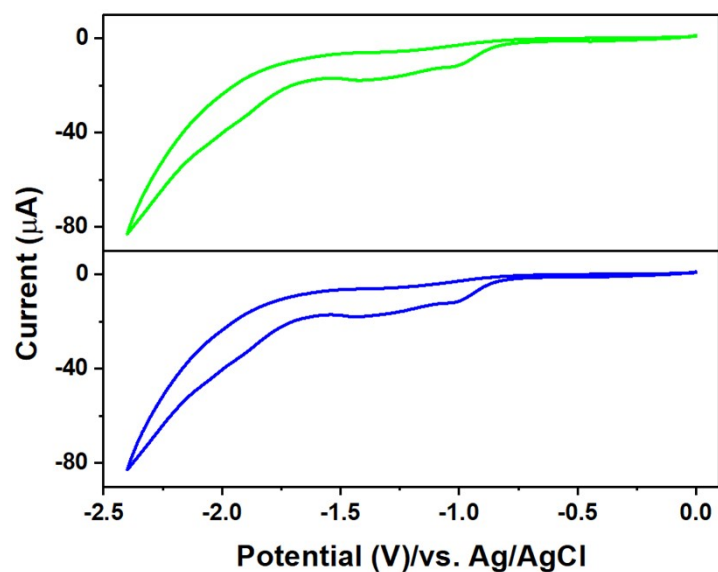


Figure S11. CV of *S*-Au₉Ag₄ (green) and *R*-Au₉Ag₄ (blue line) in degassed DCM with 0.1 M tetrabutylammonium perchlorate (TBAP) as the supporting electrolyte. A platinum disk electrode and Ag/AgCl wire were used as the working and reference electrodes, respectively. Scan rate = 0.1 V/s.

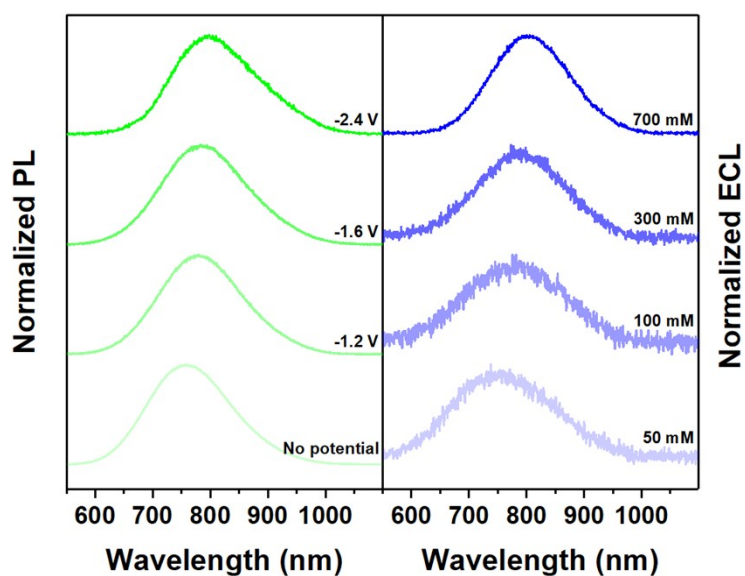


Figure S12. PL spectra of *S*-Au₉Ag₄ under various potential electrolysis conditions (left panel) and ECL spectra of *S*-Au₉Ag₄ with various concentration of TPrA coreactant (right panel).

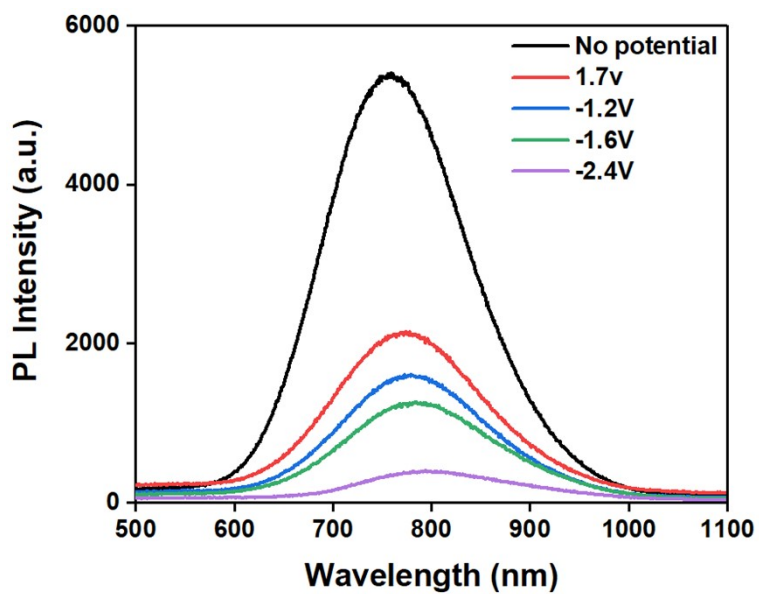


Figure S13. PL intensities of $S\text{-Au}_9\text{Ag}_4$ nanoclusters under various potential electrolysis conditions.

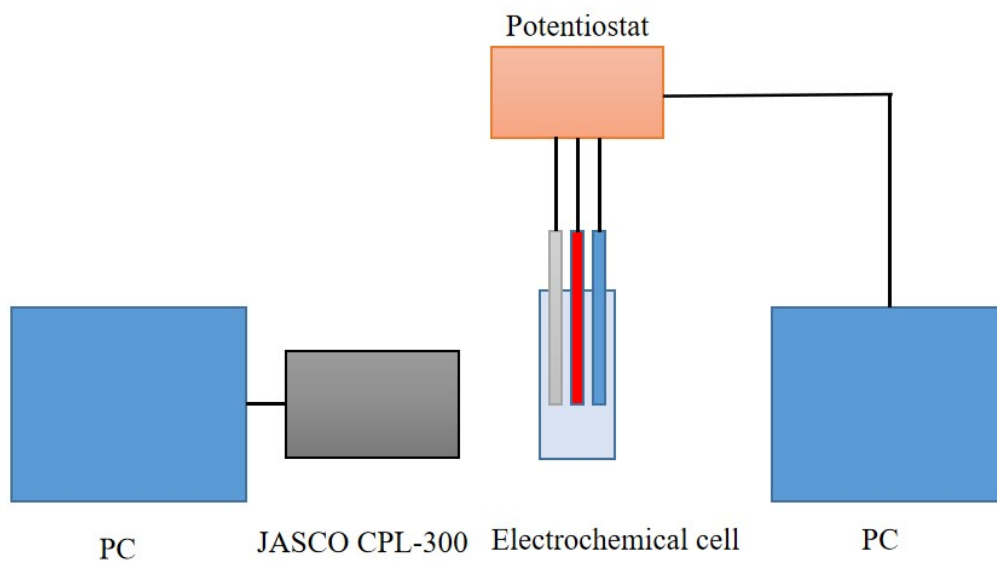


Figure S14. Diagram of apparatus for CPECL measurement with the commercial CPL instrument.

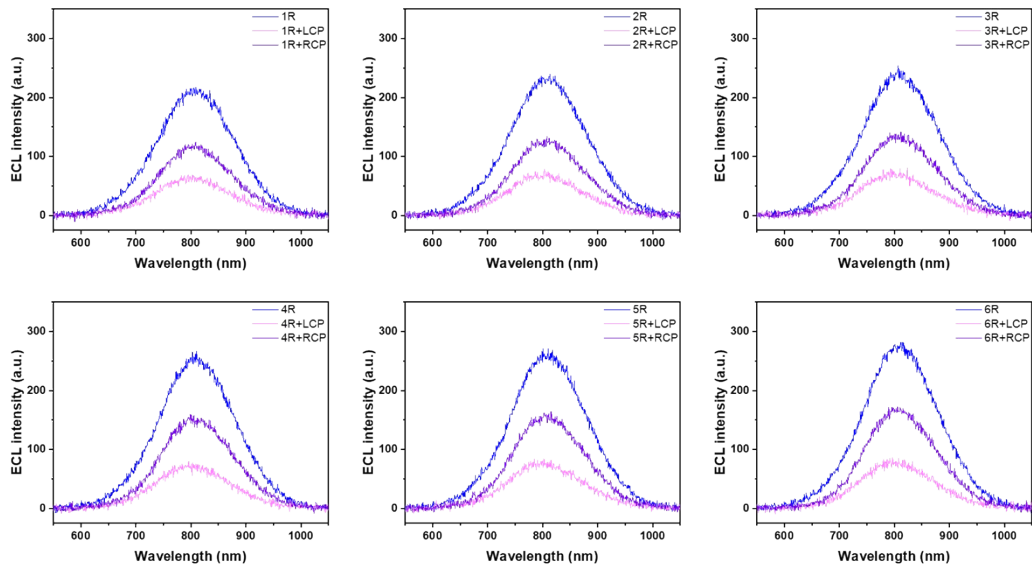


Figure S17. Six groups of ECL spectra of $R\text{-Au}_9\text{Ag}_4$ without or with CPIL808/ CPIR808 polarizer. ECL spectrum of $R\text{-Au}_9\text{Ag}_4$ without polarizer (blue), with CPIL808 polarizer (pink) and with CPIR808 polarizer (purple). The exposure time was 5s.

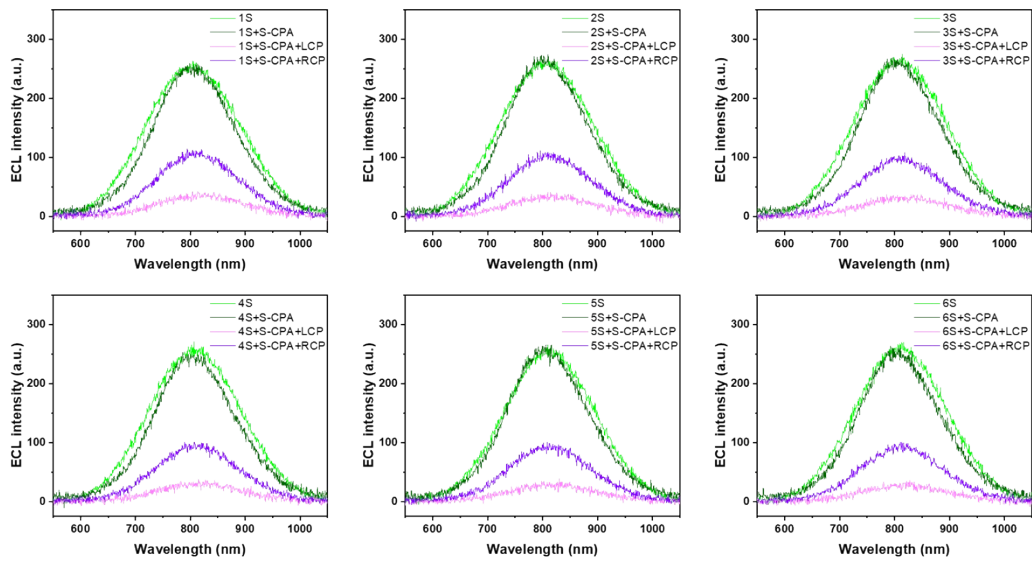


Figure S18. Six groups of ECL spectra of $S\text{-Au}_9\text{Ag}_4$ before and after adding 1 equivalent of $S\text{-CPA}$ (green and dark green lines). The spectra highlighted with pink and purple are the ECL spectra of $(S\text{-Au}_9\text{Ag}_4 + S\text{-CPA})$ with CPIL808 and CPIR808 polarizers. The exposure time was 5s.

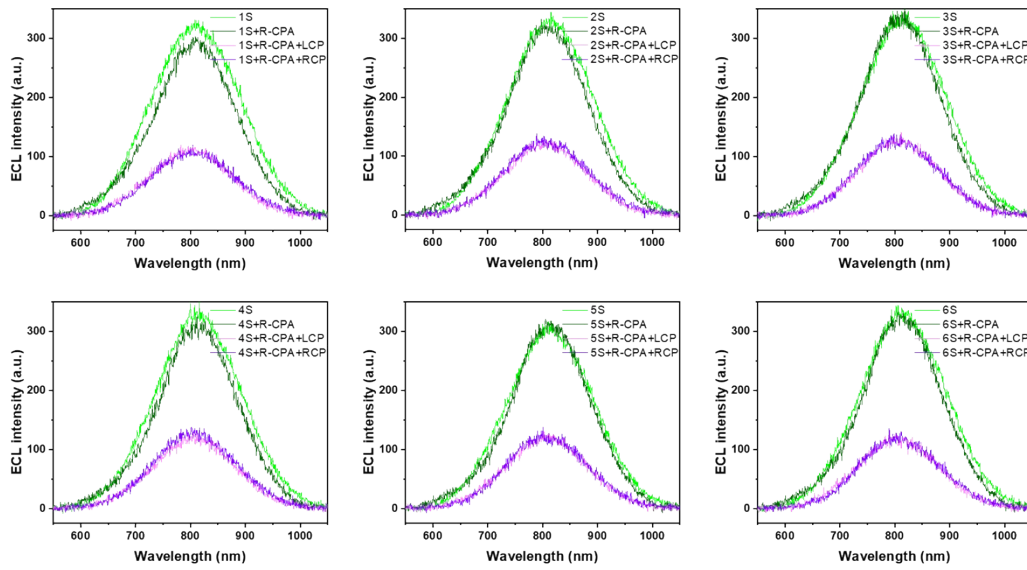


Figure S19. Six groups of ECL spectra of $S\text{-Au}_9\text{Ag}_4$ before and after adding 1 equivalent of $R\text{-CPA}$ (green and dark green lines). The spectra highlighted with pink and purple are the ECL spectra of ($S\text{-Au}_9\text{Ag}_4 + R\text{-CPA}$) with CPIL808 and CPIR808 polarizers. The exposure time was 5s.

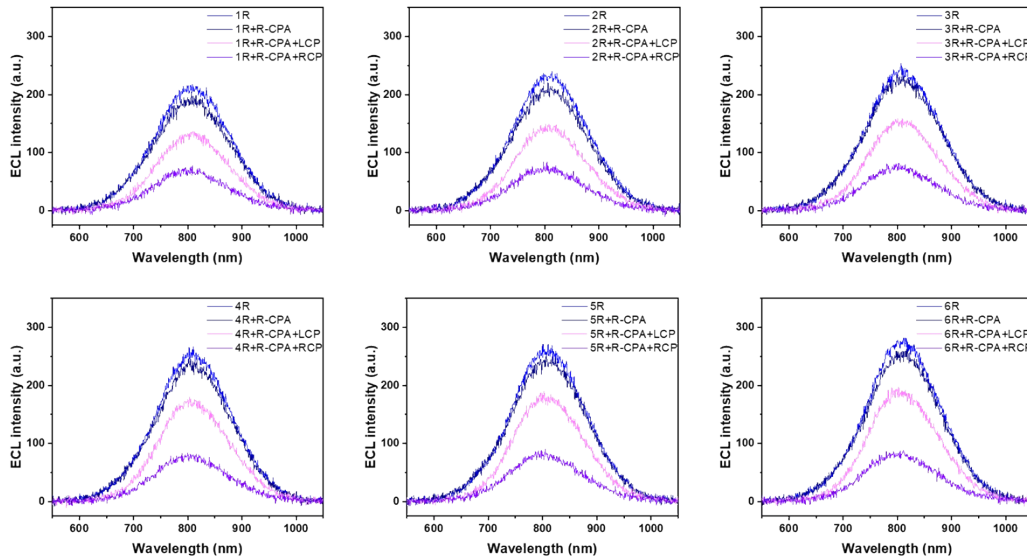


Figure S20. Six groups of ECL spectra of $R\text{-Au}_9\text{Ag}_4$ before and after adding 1 equivalent of $R\text{-CPA}$ (blue and dark blue lines). The spectra highlighted with pink and purple are the ECL spectra of ($R\text{-Au}_9\text{Ag}_4 + R\text{-CPA}$) with CPIL808 and CPIR808 polarizers. The exposure time was 5s.

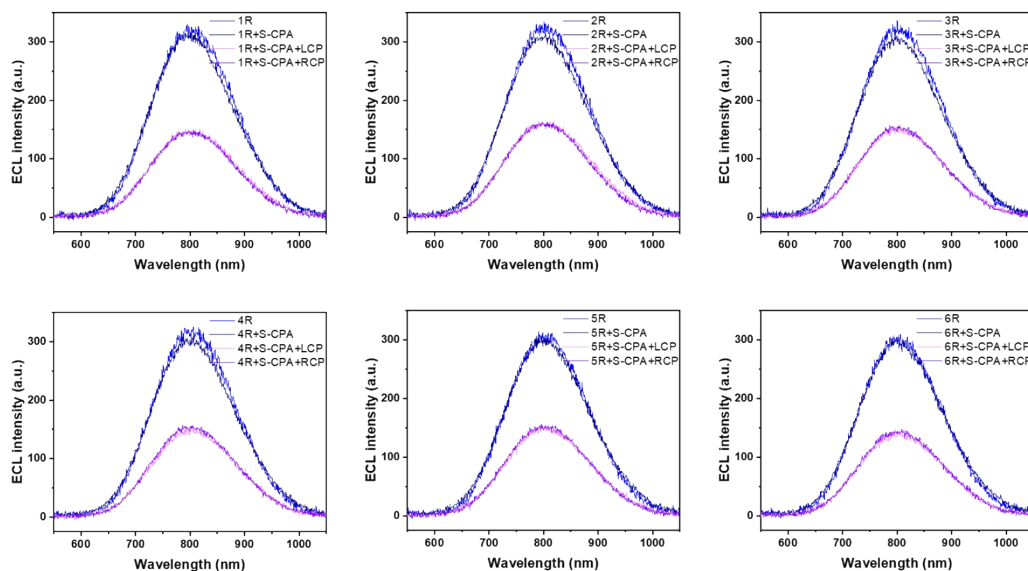


Figure S21. Six groups of ECL spectra of $R\text{-Au}_9\text{Ag}_4$ before and after adding 1 equivalent of $S\text{-CPA}$ (blue and dark blue lines). The spectra highlighted with pink and purple are the ECL spectra of $(R\text{-Au}_9\text{Ag}_4+S\text{-CPA})$ with CPIL808 and CPIR808 polarizers. The exposure time was 5s.

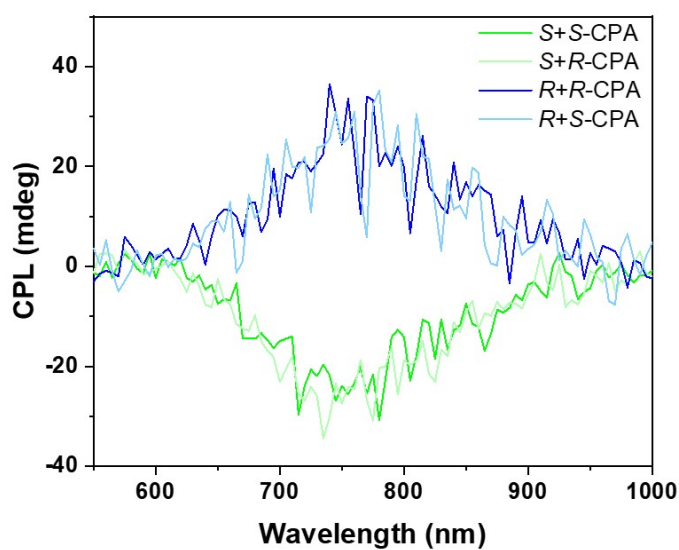


Figure S22. CPL of $S\text{-Au}_9\text{Ag}_4$ and $R\text{-Au}_9\text{Ag}_4$ after added $S\text{-CPA}$ and $R\text{-CPA}$.

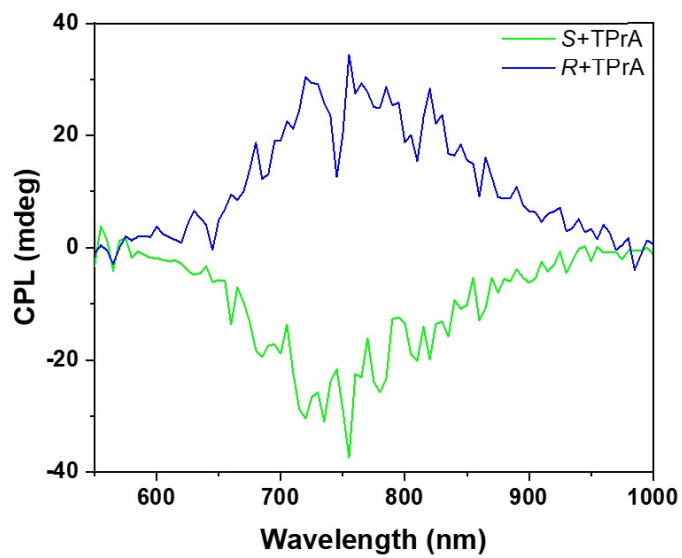


Figure S23. CPL of *S*-Au₉Ag₄ and *R*-Au₉Ag₄ after added TPrA.

Supplementary TableTable S1. Crystal data and structure refinement for [Au₉Ag₄(DPPB)₄Cl₄]Cl.

Identification code	Au ₉ Ag ₄
Empirical formula	C ₁₁₃ H ₁₁₄ Ag ₄ Au ₉ Cl ₇ P ₈
Formula weight	4172.12
Temperature/K	120
Crystal system	triclinic
Space group	P-1
a/Å	17.8906(4)
b/Å	21.6153(5)
c/Å	23.3885(5)
α/°	110.163(2)
β/°	103.825(2)
γ/°	105.043(2)
Volume/Å ³	7642.4(3)
Z	2
ρ _{calc} /cm ³	1.813
μ/mm ⁻¹	21.979
F(000)	3860.0
Radiation	CuKα (λ = 1.54186)
2θ range for data collection/°	8.462 to 139.526
Index ranges	-8 ≤ h ≤ 20, -26 ≤ k ≤ 24, -28 ≤ l ≤ 25
Reflections collected	56056
Independent reflections	27060 [R _{int} = 0.0466, R _{sigma} = 0.0430]
Data/restraints/parameters	27060/45/1270
Goodness-of-fit on F ²	1.037
Final R indexes [I >= 2σ (I)]	R ₁ = 0.0882, wR ₂ = 0.2493
Final R indexes [all data]	R ₁ = 0.0992, wR ₂ = 0.2690
Largest diff. peak/hole / e Å ⁻³	6.84/-4.64